



EUROfusion

EUROFUSION WPMST2-CP(16) 15473

D.E. Aguiam et al.

X-mode raw data analysis of the new AUG ICRF antenna edge density profile reflectometer

Preprint of Paper to be submitted for publication in
Proceedings of 29th Symposium on Fusion Technology (SOFT
2016)



This work has been carried out within the framework of the EUROfusion Consortium and has received funding from the Euratom research and training programme 2014-2018 under grant agreement No 633053. The views and opinions expressed herein do not necessarily reflect those of the European Commission.

This document is intended for publication in the open literature. It is made available on the clear understanding that it may not be further circulated and extracts or references may not be published prior to publication of the original when applicable, or without the consent of the Publications Officer, EUROfusion Programme Management Unit, Culham Science Centre, Abingdon, Oxon, OX14 3DB, UK or e-mail Publications.Officer@euro-fusion.org

Enquiries about Copyright and reproduction should be addressed to the Publications Officer, EUROfusion Programme Management Unit, Culham Science Centre, Abingdon, Oxon, OX14 3DB, UK or e-mail Publications.Officer@euro-fusion.org

The contents of this preprint and all other EUROfusion Preprints, Reports and Conference Papers are available to view online free at <http://www.euro-fusionscipub.org>. This site has full search facilities and e-mail alert options. In the JET specific papers the diagrams contained within the PDFs on this site are hyperlinked

X-mode raw data analysis of the new AUG ICRF antenna edge density profile reflectometer

D.E. Aguiam^a, A. Silva^a, V. Bobkov^b, P.J. Carvalho^a, P.F. Carvalho^a, R. Cavazzana^c, G.D. Conway^b, O. D’Arcangelo^d, L. Fattorini^e, H. Faugel^b, A. Fernandes^a, H. Fünfgelder^b, B. Goncalves^a, L. Guimaraes^a, G. De Masi, L. Meneses^a, J.M. Noterdaeme^{b,f}, R.C. Pereira^a, G. Rocchi^d, J.M. Santos^a, A.A. Tuccillo^d, O. Tudisco^d, ASDEX Upgrade Team^b

^a*Instituto de Plasmas e Fusão Nuclear, Instituto Superior Técnico, Universidade de Lisboa, 1049-001 Lisboa, Portugal*

^b*Max-Planck-Institut für Plasmaphysik, Boltzmannstr. 2, D-85748 Garching, Germany*

^c*Consorzio RFX (CNR, ENEA, INFN, Università di Padova, Acciaierie Venete SpA), Corso Stati Uniti 4, 35127 Padova, Italy*

^d*ENEA, Dipartimento FSN, C. R. Frascati, via E. Fermi 45, 00044 Frascati (Roma), Italy*

^e*Università degli Studi Milano Bicocca, dipartimento di Fisica, piazza della Scienza 3, 20126 Milano, Italy*

^f*Ghent University, Applied Physics Department, B-9000 Gent, Belgium*

Abstract

The new multichannel X-mode reflectometer installed on ASDEX Upgrade measures the plasma density profile evolution at different positions in front of the ICRF antenna. The reflectometer operates in the extended U-band (40-68 GHz) microwave region, measuring density profiles up to $2 \times 10^{19} \text{ m}^{-3}$ with magnetic fields between 1.5 T and 2.7 T. In this heterodyne reflectometer architecture, the signal reflected by the plasma is down-shifted to a lower intermediate frequency, amplified and filtered with a 100 MHz bandpass filter. Quadrature detectors demodulate the in-phase and quadrature (IQ) signals, which are acquired at 200 MS/s. In this work we analysed the acquired IQ signals from the different reflectometer antennas, and describe the waveguide dispersion calibration and filtering of the raw signal. The effect of spurious reflections, such as the multiple reflections from the ICRF antenna metal straps, are analysed and taken into account on the data processing software. In some high plasma density and high magnetic field scenarios, both the lower and upper X-mode cut off frequencies are detected in the probing U-band. The first fringe reflection of the upper cut off indicates the beginning of the plasma signal and must be determined robustly to reduce density profile errors. A moving persistence window algorithm is used for consecutive sweeps to improve the group delay signal used for electron density profile inversion.

1. Introduction

A new multichannel X-mode edge density profile reflectometer was installed on ASDEX Upgrade (AUG) and commissioned during the 2015-2016 operational campaign. This frequency modulated continuous wave reflectometry diagnostic has heterodyne detection and was designed to use three of the ten available bistatic microwave antennas. These bistatic antennas are embedded at different locations of the ICRF (Ion Cyclotron Range of Frequencies) antenna and have independent vacuum feed-through and transmission lines. The plasma is probed in the extended 40 to 68 GHz U-band region, measuring density profiles up to $2 \times 10^{19} \text{ m}^{-3}$ with magnetic fields between 1.5 T and 2.7 T and a temporal resolution of 100 μs [1].

The successful operation of a reflectometry diagnostic is greatly dependent on proper calibration during maintenance phase, when access inside the vessel is possible, but also on the correct interpretation of the acquired raw signals. The microwave components’ response, the waveguide dispersion, and even the effect of metallic structures inside the vessel, can all be observed in the acquired signal alongside the plasma reflection signal. Their contributions must be understood to obtain the cleanest group delay signal possible from which the density

profiles are processed.

In this work, the different steps to calibrate and filter the heterodyne reflectometry raw signals are presented. The X-mode propagation response is analysed to determine the upper and lower cut off regions and obtain the group delay used for density profile inversion.

2. Reflectometry architecture and raw signal

The plasma refractive index N of an electromagnetic wave with frequency f propagating in X-mode, where its electric field is perpendicular to the magnetic field, is given by

$$N_X^2(f, r) = 1 - \frac{f_{pe}^2(r) \left(1 - \frac{f_{pe}^2(r)}{f^2}\right)}{f^2 - f_{pe}^2(r) - f_{ce}^2(r)}, \quad (1)$$

where $f_{pe}^2(r) = n_e(r) e^2 / (4\pi\epsilon_0 m_e)$ is the electron plasma frequency, dependent on the electron density n_e , and $f_{ce}(r) = eB(r) / (2\pi m_e)$ is the electron cyclotron frequency, where B is the local magnetic field. Solving $N_X \rightarrow 0$, for given n_e and B values, gives two frequency solutions above and below f_{ce} , respectively called the upper and lower cut off frequencies, at which the wave is reflected.

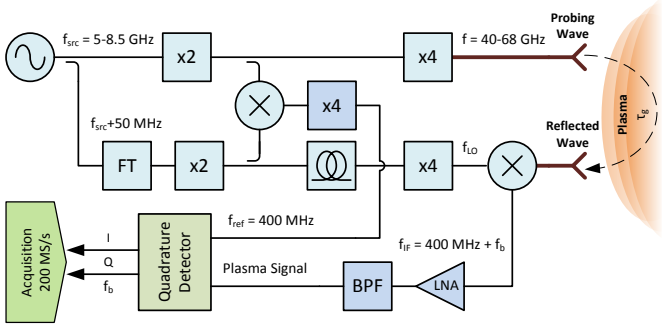


Figure 1: Heterodyne topology of the reflectometer. A single oscillator generates the source signal. Frequency doublers ($\times 2$) and quadruplers ($\times 4$) are used to generate the output probing and reference (LO) signals. A frequency translator (FT) introduces a 50 MHz offset in the source reference signal that is up shifted to a 400 MHz frequency shift in the LO signal. Further details can be found in [1].

This reflectometry diagnostic was designed with a full coherent heterodyne architecture (see Figure 1) to use the X-mode upper cut off region to measure edge plasma electron density profiles.

A probing wave, with a linearly swept frequency f between 40 and 68 GHz in $15 \mu\text{s}$, is launched into the plasma and is reflected at a cut off electron density layer, which depends on the wave frequency and the local magnetic field. The propagation of this probing wave through the waveguides and through the plasma introduces a delay τ that depends on the waveguide dispersion and the plasma density profile. When mixing the reflected signal with a synchronized frequency shifted reference local oscillator signal (LO), at f_{LO} , a band pass filtered (BPF) intermediate frequency (IF) signal is obtained. The IF signal includes a beat signal, with a bandwidth of 100 MHz, centred at 400 MHz. The quadrature detector uses a 400 MHz reference to downshift and convert the IF signal into its in-phase and quadrature (IQ) components. The baseband beat signal frequency f_b is proportional to the round-trip probing wave group delay τ and the sweep rate df/dt :

$$f_b = \tau \frac{df}{dt}. \quad (2)$$

Figure 2 shows an uncalibrated raw signal acquired in a plasma discharge with high magnetic field and high electron density. The amplitude and phase of the signal are calculated using the raw signal IQ components. A short-time Fourier transform (STFT) algorithm processes the complex raw signal, $I - iQ$, to represent the beat frequency evolution, or group delay evolution, against the probing frequency. The beat frequencies of the maximum amplitude peaks of the STFT correspond to the signal result of the plasma reflection. Other peaks, such as multiple reflections between the plasma reflection layer and the metal vessel walls, may appear and must be filtered.

In this example, it can be concluded that the X-mode lower cut off region goes up to 52 GHz and that the first fringe reflection of the upper cut off region, corresponding to $n_e \approx 0$, occurs somewhere in the 52-56 GHz range. A multiple reflection signal, distorting the main reflection signal, occurs near the

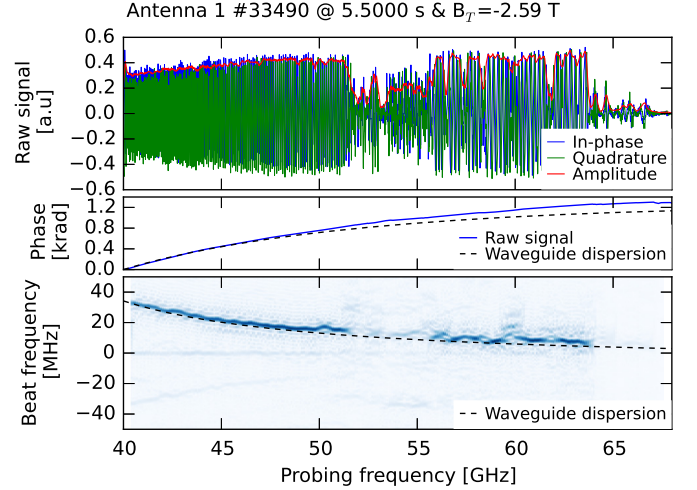


Figure 2: Representation of the uncalibrated raw beat frequency signal measured during a discharge with plasma.

60 GHz. Also, both the low power output of the front end $\times 4$ multipliers and the conversion losses of the front end mixers towards the end of the U-band region result in a low signal amplitude in the 64-68 GHz region, which limits the useful probing region up to 64 GHz.

3. Calibration of waveguide dispersion

The reflectometer front-ends are separated from the in-vessel antennas by over 10 m of WR19 waveguides. The waveguide dispersion introduces a group delay in the probing wave propagation that decreases non-linearly as a function of the wave frequency. The group delay introduced by the waveguide results in an added phase ϕ_{wg} shift to the raw signal. By calculating what this phase contribution is and removing it from the raw signal, a calibrated signal is achieved.

For the waveguide calibration, a metallic mirror was placed at several distances in front of each reflectometry channel antenna pair, and the reflectometer beat frequency signals were acquired. The same STFT algorithm was used to determine the group delay vs probing frequency response. The vacuum propagation contribution to the group delay was removed and the average response of all the mirror distances was fitted to the group delay function[2]:

$$\tau_{wg} = a + \frac{b}{\sqrt{1 - \left(\frac{f_c}{f}\right)^2}}, \quad (3)$$

where a includes the contribution of any constant delay introduced by the microwave components and connections inside the reflectometer, b the contribution of waveguide length, and f_c is the lower order cut off frequency of the waveguide. For the range of probing frequencies, the waveguide group delay $\tau_{wg}(f(n))$ and beat frequency $f_{b_{wg}}(f(n))$ responses are reconstructed. The phase $\phi_{wg}(n)$ is calculated as:

$$\phi_{wg}(n) = \sum_{n_i=0}^n f_{b_{wg}}(f(n_i)) \frac{2\pi}{f_s} \quad (4)$$

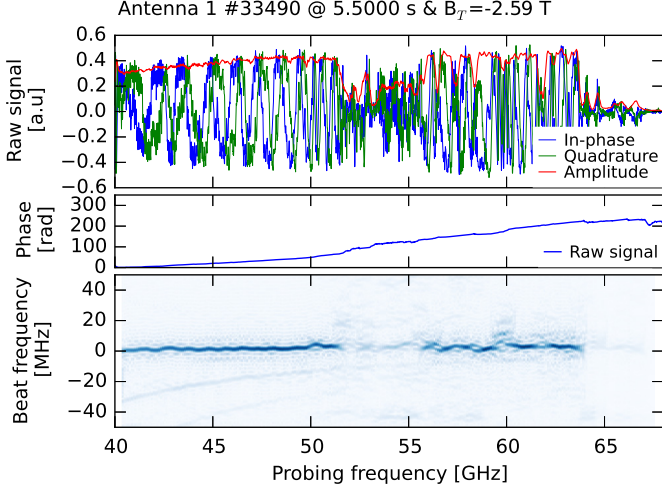


Figure 3: Representation of the calibrated linearised beat frequency signal during a discharge with plasma.

where f_s is the sampling frequency. The reconstructed beat frequency and phase responses of the waveguide contribution can also be observed in Figure 2.

A complex signal, such as the $sig(n) = I(n) - iQ(n)$ raw signal can be represented in the exponential form:

$$sig(n) = A(n) e^{i\phi(n)}, \quad (5)$$

$$A(n) = \sqrt{I^2(n) + Q^2(n)} \quad \text{and} \quad \phi(n) = \tan^{-1} \left(\frac{Q(n)}{I(n)} \right). \quad (6)$$

By removing the waveguide dispersion contribution to the phase, assuming an unitary amplitude, the calibrated signal can be numerically reconstructed:

$$sig_{cal}(n) = A(n) e^{i(\phi(n) - \phi_{wg}(n))}. \quad (7)$$

With this, the linearised calibrated signal depends mostly on the plasma in front of the reflectometry antennas, though some undesired effects, such as multiple reflections due to the Faraday straps of the ICRF antenna, may still show up at higher frequencies in the signal and must be filtered. The resulting calibrated signal and STFT response are represented in Figure 3.

The raw signal is digitally filtered in two steps. Long cable connections between the reflectometer and the acquisition system may pick up a low frequency signal which is removed by a high pass filter before the calibration procedure. The calibration procedure linearises the plasma beat frequency signal and allows a second low pass filter to limit the signal to the region of interest, removing the higher frequency multiple reflections.

4. Estimation of X-mode reflectometry group delay

Microwave reflectometry electron density profiles can be determined from the frequency dependence of the phase delay $\phi(\omega)$ of the reflected wave, which is calculated from the group delay measurement at each probing frequency [3]. The X-mode reflectometry reflection signal greatly depends on experiment

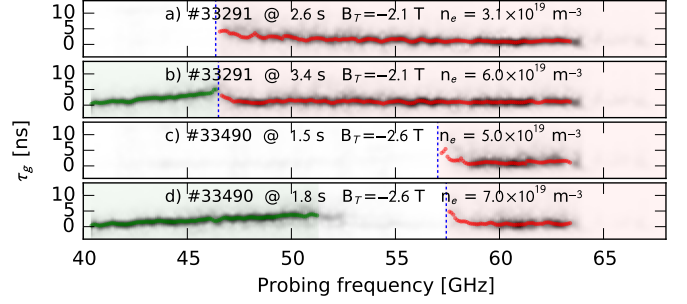


Figure 4: Different electron density and magnetic field scenarios and resulting reflectometry of Antenna 1. The X-mode upper cut off (red) and lower cut off (green) regions are represented, along with the estimated group delay. The first fringe reflection frequency of each scenario is represented by the vertical dashed line, indicating the start of the upper cut off region.

conditions, which must be studied to extract the correct group delay information. The measured group delays in different magnetic field and plasma electron density scenarios are shown in Figure 4.

By design, the first fringe reflection (FF) indicating the start of the upper cut off region, may occur anywhere in the 40-68 GHz U-band probing window. A higher magnetic field results in shift of the FF towards the end of the U-band, shortening the probeable plasma region, as can be observed in Figure 4 a) and c), where the FF is represented by the vertical dashed line.

However, a higher core plasma electron density may also result in a lower cut off reflection that extends into the probing window, as observed in Figure 4 b) and d). This lower cut off region extends gradually as the density increases, as noted between c) and d), and may even overlap with the upper region, as seen in b). Despite this overlap, the probing wave is reflected at the first cut off layer it encounters, which, considering a monotonically increasing density profile, occurs in the outer layers. For this reason, the upper cut off reflection will always prevail in the measured response.

While the large window size and zero padding techniques used in the STFT allow for a group delay resolution of around 0.05 ns, it is also necessary to improve the quality of the plasma reflection signal in order to prevent signal power gaps and distortions that may arise due fast plasma events, such as turbulence or edge localized modes (ELM). For this purpose a persistence method on the STFT result matrices is used, where the P previous sweeps are averaged. This results in an accumulation of the common reflection features in consecutive acquisitions, while diluting the effect of sporadic signal jitter. As observed in Figure 5 1) to 6), the obtained group delays become cleaner with the increase of P , showing the time smoothed fine structure of the plasma. Although this reduces the temporal resolution T of the measured profiles, a moving persistence window is used so that transient events may be observed with a maximum $P \times T$ delay, as seen in Figure 5 6) to 8).

The group delay is then obtained from the STFT result at the maximum peak of each probing frequency in the upper cut off region, after the first fringe reflection. The density profiles are processed from the group delay according to the X-mode inversion algorithm described in [3].

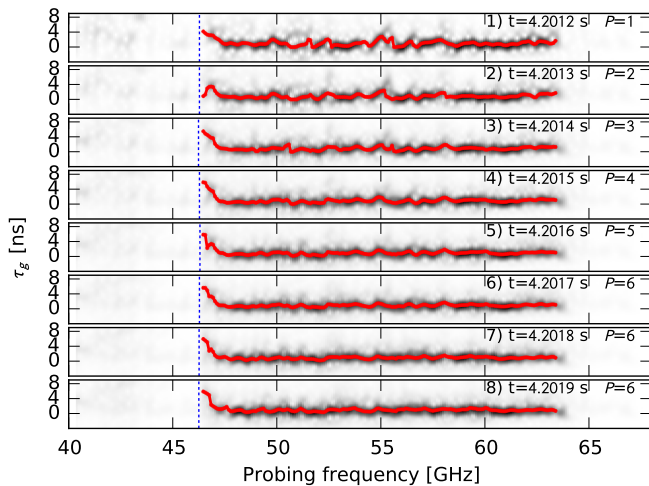


Figure 5: Group delay measurements of Antenna 1 during discharge #33291 using the moving persistence window method for different persistence P values.

5. Density profile measurements

An example density profile evolution during 13 ms with the occurrence of an ELM event was calculated and is represented in Figure 6, in poloidal flux coordinates with a time resolution of $100 \mu\text{s}$. The core electron density was $7.4 \times 10^{19} \text{ m}^{-3}$ with $B_T = -2.5 \text{ T}$. During an ELM event there is a relaxation of the density profile, resulting in the outwards expansion of the lower densities, as can be observed in Figure 6. The high magnetic field limits the maximum measurable density to around $0.7 \times 10^{19} \text{ m}^{-3}$, not enough to reach the separatrix, but still allowing the observation of ELM effects on the outer plasma edge.

The moving persistence window method results in smooth density gradients and still allows the observation of fast transients in the profile gradient.

One important aspect to consider in X-mode density profile reflectometry, is its dependency on the magnetic equilibrium reconstruction. Besides the magnetic equilibrium being used to invert the density profiles, it is also used to calculate the vacuum distance between the reflectometry antenna and the start of the plasma, which must be removed from the group delay measurements.

The start of the plasma r_p is considered to occur at the first fringe reflection of the upper cut off region. By assuming $n_e \approx 0$, then the FF frequency equals that of the local cyclotron frequency, provided by the magnetic equilibrium: $f_{FF} = f_{ce}(r_p)$. In reality, the first reflection occurs at a residual density layer, which must be considered when calculating r_p .

A wrong estimation of the FF results in a radial error, due to incorrect estimation of the vacuum distance, and in density gradient errors, as vacuum propagation delay error is integrated along the profile.

In addition, the first fringe reflection usually varies throughout the discharge, and may even vary faster than the 1 ms time resolution of the magnetic equilibrium reconstruction. For this reason, a reliable FF estimation algorithm that is capable of determining and tracking the start of the X-mode upper cut off reflection in any scenario along the discharge must be used.

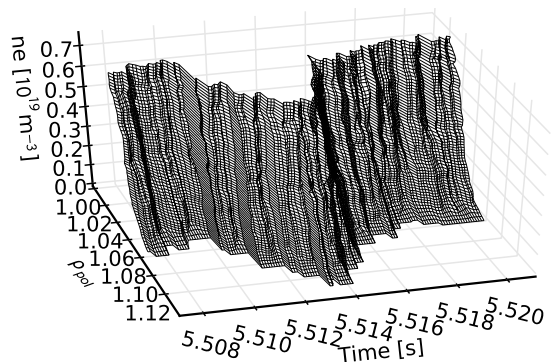


Figure 6: Time evolution of edge electron density profiles during an ELM event measured at Antenna 4 during discharge #33214

6. Summary and conclusions

In this work it was shown that the acquired reflectometry raw signal must be properly interpreted in all operation conditions to correctly estimate the reflection wave group delays required to process the density profile. The calibration procedure to remove the waveguide propagation contribution to the group delay was presented and the different operation scenarios, specific to X-mode reflectometry, were explained. Signal quality may be improved by averaging consecutive acquisitions and accentuating the common features. The magnetic field used during the discharge sets the upper limit for the density profile measurement. A robust first fringe reflection estimation algorithm must be used to track the start of the X-mode upper cut off region to avoid group delay errors due to vacuum propagation. The diagnostic was demonstrated to be capable of presenting detailed density profiles during ELM events.

Acknowledgements

This work has been carried out within the framework of the EUROfusion Consortium and has received funding from the Euratom research and training programme 2014-2018 under grant agreement No 633053. IST activities also received financial support from Fundação para a Ciência e Tecnologia through project UID/FIS/50010/2013 and the PhD Scholarship FCT-SFRH/BD/52414/2013. The views and opinions expressed herein do not necessarily reflect those of the European Commission.

References

- [1] D. E. Aguiam, A. Silva, V. Bobkov, P. J. Carvalho, P. F. Carvalho, R. Cavazzana, G. D. Conway, O. Darcangelo, H. Faugel, A. Fernandes, B. Goncalves, L. Guimaraes, G. De Masi, L. Meneses, J. M. Noterdaeme, R. C. Pereira, G. Rocchi, J. M. Santos, A. A. Tuccillo, O. Tudisco, t. A. U. Team, Implementation of the new multichannel X-mode edge density profile reflectometer for the ICRF antenna on ASDEX Upgrade, Submitted to Review of Scientific Instruments (Submitted).
- [2] A. F. Harvey, Microwave engineering, 2nd Edition, Academic Press Inc. (London) Ltd., 1963.
- [3] E. Mazzucato, Microwave reflectometry for magnetically confined plasmas, Review of Scientific Instruments 69 (1998) 2201. doi:10.1063/1.1149121.